JOURNAL OF APPLIED POLYMER SCIENCE VOL. 15, PP. 2395–2415 (1971)

Rheological and Heat Transfer Aspects of the Melt Spinning of Monofilament Fibers of Polyethylene and Polystyrene

DOMENICO ACIERNO,* J. NELSON DALTON,† JORGE M. RODRIGUEZ, and JAMES L. WHITE,** *Department of Chemical and Metallurgical Engineering, University of Tennessee, Knoxville, Tennessee 37916*

Synopsis

Two experimental studies of the melt spinning of fibers have been carried out using low-density polyethylene and polystyrene. First, isothermal spinning experiments were carried out and the relationship between the fiber kinematics and drawdown force was studied. The data were correlated by using the following two methods: (1) the concept of a non-Newtonian elongational viscosity and (2) a nonlinear integral theory of viscoelastic fluids. In the second experiment, the spinline temperature profile of a monofilament fiber being pulled down from a spinneret through stagnant air was measured and the heat transfer coefficient computed. A correlation between the local Nusselt number and a fiber Reynolds number was obtained. An integral boundary layer analysis of forced convection heat transfer from a descending fiber was carried out.

INTRODUCTION

In the years since the development of the melt spinning method of manufacturing fibers by Carothers, Hill, Bolton and their colleagues of the du Pont Company,[1,2] a great industry has grown about the process. Through the years most research in this area has been oriented toward product development, and only in the past decade has attention been given to attempting to quantitatively understanding the melt spinning process. The publications of Ziabicki and his associates[3,4] in 1960–61 did much to open up this area and have exerted a strong influence since that time.

Fundamental research on melt spinning may be divided into two categories involving the investigation of (1) rheological phenomena and heat transfer in the upper part of the spinline near the spinneret, and (2) structure formation, specifically orientation and crystallinity in the middle and lower parts of the spinline. Experimental studies of the former problem have been carried out by Ziabicki,[3,4] Kase and Matsuo,[5] Wilhelm,[6] and

* Present address: Research Laboratory for Technological Research in Polymers and Rheology, Consiglio Nazionale delle Ricerche, Naples, Italy.

† Present address: Tennessee Eastman Company, Kingsport, Tennessee.

** To whom all communications should be addressed.

Ishibashii, Aoki, and Ishii.[7] Consideration of the rheological characteristics have generally followed the classical analyses of stretching of Newtonian fluids by Trouton,[8,9] only with the additional complication that the tensile viscosity is temperature dependent. Some efforts have been made in the direction of considering the non-Newtonian characteristics of the melts. Ballman[10] and Cogswell[11] have attempted to measure tensile viscosities of melts, while White,[12] Matovich and Pearson,[13] and Han,[14] among others, have published theoretical analyses showing the significance of non-Newtonian effects in spinning. Studies of the variation of birefringence, density, and x-ray orientation factor of fibers spun under different conditions have appeared in the literature, as have variations of birefringence along the spinline.[7,15,16] A recent study of Katayama, Amano, and Nakamura[16] has utilized a new x-ray technique to investigate the variation of crystal structure along the spinline. Ziabicki[17,18] has attempted to model the entire fiber spinning process, including structure formation. This author has also provided a critical review of much of the earlier literature.[18]

It is the purpose of this paper to present a critical study of the rheological and heat transport characteristics of fibers in the upper part of the spinline. The paper is divided into two sections; the first part considers fiber spinning under isothermal conditions, and in the second part the temperature profile along the spinline is evaluated and a heat transfer correlation is developed. Our reason for studying isothermal spinning is that the presence of large temperature gradients masks the detailed rheology and allows correlation of experimental data with almost any expression containing arbitrary temperature-dependent coefficients. This research project on our part represents an extension of our group's studies of the flow of melts in capillary dies.[19–21]

ISOTHERMAL SPINNING

Theoretical Analysis

If we make a force balance between an arbitrary position x (measured from the spinneret) in a fiber spinline and a position L, which may be the position of the take-up device or simply represent where the force F_L is measured, we may write[3,12,18]

$$\int_0^{R(L)} 2\pi r\rho V^2 dr - \int_0^{R(x)} 2\pi r\rho V^2 dr = F_L + F_{\text{grav}} - F_{\text{drag}} - F_{\text{surf}} - F_x \tag{1}$$

where F_{grav} is the gravitational force pulling the fiber downward, F_{drag} is the frictional drag of the ambient air on the surface of the fiber, F_{surf} is the surface tension force, and F_x is the tensile force within the fiber at position x. As generally all of the quantities except F_x are known, eq. (1) may be used to calculate the tensile forces within the melt. In particular,

if we presume a flat velocity field within the moving filament, we may write

$$F_x = \pi R^2(x)\sigma_{xx}(x) = F_L + \int_x^L [\rho g \pi R^2(\xi) - 2\pi R(\xi)\sigma_{rx}\Big|_{\text{surf}}]d\xi - F_{\text{surf}} - \rho Q^2\left[\frac{A(x) - A(L)}{A(x)A(L)}\right] \quad (2)$$

wherein Q is the volumetric flow rate and $A(x)$ is the cross-sectional area at position x, i.e., $\pi R^2(x)$.

If an expression for $\sigma_{xx}(x)$ is available, it will then be possible to predict the variation of $R(x)$ or $A(x)$ with distance along the length of the descending fiber. Alternatively, one might use experimental data for $A(x)$ versus x to compute $\sigma_{xx}(x)$. One would also be able to then express σ_{xx} as a function of the deformation processes in the spinline. It is this approach that we will take here.

If the melt being spun may be considered to be a Newtonian fluid, i.e., its constitutive equation has the form[22]

$$\sigma_{ij} = -p\delta_{ij} + \eta\left[\frac{\partial V_i}{\partial x_j} + \frac{\partial V_j}{\partial x_i}\right], \quad (3a)$$

then

$$\sigma_{xx}(x) = 3\eta\frac{dV}{dx} = 3\eta\frac{d}{dx}\left[\frac{Q}{A(x)}\right]. \quad (3b)$$

Knowledge of dV/dx and the shear viscosity should allow us to compute the profile of tensile stress versus axial distance.

On the other hand, if the melt is viscoelastic, i.e., the stress depends upon the history of the deformation,[23] then

$$\sigma_{ij} = -p\delta_{ij} + F_{ij}\left[\overset{s=t}{\underset{s=-\infty}{e_m(t-s)}}\right] \quad (4a)$$

with e_{mn} being a suitable strain tensor. E.g.,

$$e_{ij} = \left(\frac{1}{2}\right)\left[\frac{\partial x_i}{\partial \bar{x}_a}\frac{\partial x_j}{\partial \bar{x}_a} - \delta_{ij}\right] \quad (4b)$$

where $\bar{x}_a$ are the Cartesian coordinates of a material point in the fiber at times s, and x_i, at time t. For a long-duration steady extension flow with constant axial velocity gradient, the strain tensor may be expressed in a Rivlin-Ericksen expansion and the stress $\sigma_{xx}(x)$ can be written[24]

$$\sigma_{xx}(s) = \chi\frac{dV}{dx} \quad (5a)$$

where χ is an elongational viscosity which depends upon the axial velocity gradient. For small dV/dx we have

$$\lim_{\frac{dV}{dx}\to 0}\chi = 3\left[\int_0^\infty G(s)ds\right] = 3\eta \quad (5b)$$

where η is the zero shear viscosity and $G(s)$ is the relaxation modulus of linear viscoelasticity. If dV/dx varies slowly with x, an expression of the form of eq. (5a) will still be valid.

If the period of deformation is small or if the variations in dV/dx relative to the characteristic time λ_{ch} (e.g., maximum relaxation time) are large, no such simplification of eq. (4) will be possible, and the functional F_{ij} must be expressed in terms of integrals of e_{mn} and the deformation history substituted. (Compare the remarks of Metzner, White and Denn.[25]) For any of the realistic constitutive equations utilized to represent polymer melts,[23,25,26] the results would be indeed very complex. However, for relatively small axial velocity gradients, the problem may be simplified by using an asymptotic form of F_{ij}. A reasonable approximation for low deformation rates and small deformations is the so-called Lodge fluid,[29,30] which represents a sort of second-order correction to linear viscoelasticity theory (see our earlier remarks on this[23,31]). Lodge's equation is of the form

$$F_{ij} = 2\int_{-\infty}^{t} \phi(t - s)e_{ij}(s)ds \tag{6}$$

where $\phi(t)$ is $(-dG(t)/dt)$ and is thus uniquely determinable from linear viscoelastic data.

In order to compute $\sigma_{xx}(x)$ for a Lodge fluid, we must specify the kinematics. If we presume that a virgin melt emerges from the die and moves vertically downward with a flat velocity profile, the deformation may be thought of in terms of the uniaxial extension of a cylinder of initial cross-sectional area $A(0)$ and differential thickness. It may readily be shown that

$$\begin{aligned}\sigma_{xx}(x) &= \int_{s=-\infty}^{s=t} \phi(t - s)\left[\frac{A^2(s)}{A^2(t)} - \frac{A(t)}{A(s)}\right]ds \\ &= \int_{s=0}^{s=t} G(t - s)\frac{d}{d(t - s)}\left[\frac{A^2(s)}{A^2(t)} - \frac{A(t)}{A(s)}\right]ds \end{aligned} \tag{7}$$

where $A(s)$ is the cross-sectional area of the filament at a time s after the same material particles exit the die. (Note that $\alpha(s)A(s)$, where $\alpha(s)$ is the effective extension ratio of the differential material cylinder, is constant during the descent.) If $G(t)$ and the kinematics are known, $\sigma_{xx}(x)$ may be computed.

A weakness in the analysis of the above paragraph is that it presumes that the melt does not remember the high shearing rates in the capillary and the converging flow in the reservoir preceding the capillary. This is, of course, not the case, and it is possible to take this type of situation into consideration.[32] Let us divide the integral of eq. (6) into two parts, one considering capillary shearing from time $-\infty$ to time 0 and the second

considering extensional flow from time 0 to time t. To a first approximation, it may be shown that, at time t and position x,

$$\sigma_{xx}(x) = \sigma_{xx}(0)\left[\frac{\int_t^\infty sG(s)ds}{\int_0^\infty sG(s)ds}\right] + \int_0^t G(t-s)\frac{d}{d(t-s)} \times \left[\frac{A^2(s)}{A^2(t)} - \frac{A(t)}{A(s)}\right]ds. \quad (8)$$

EXPERIMENTAL

Materials

Low-density polyethylene (Dow 560 E) and polystyrene (Dow experimental polymer) were used in this study. Gel permeation chromatography

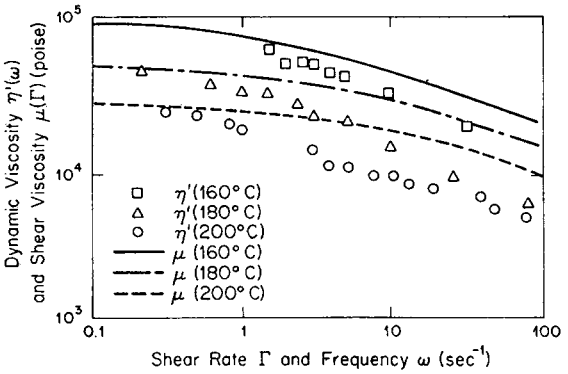

Fig. 1. Shear viscosity $\mu(\Gamma)$ and dynamic $\eta^1(\omega)$ for low-density polyethylene.

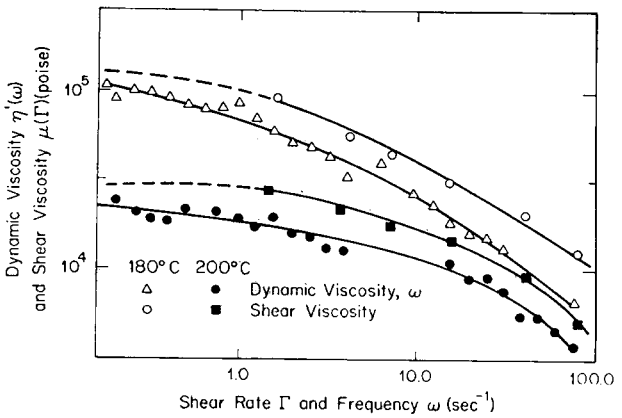

Fig. 2. Dynamic viscosity vs. frequency and shear viscosity vs. shear rate for polystyrene, 180°C and 200°C.

was used to evaluate the molecular weight distribution of the polystyrene. The number-average molecular weight was found to be 48,000 and the weight-average, molecular weight 188,000.[33] The GPC unit had been calibrated with polystyrene standards. The density of the polyethylene at room temperature was 0.92 g/cm^3 and that of the polystyrene, 1.02 g/cm^3. Shear viscosities were determined on these melts in an Instron capillary rheometer (high shear rates) and a Weissenberg rheogoniometer (low shear rates). Dynamic viscosities were also obtained on the Weissenberg rheogoniometer using an oscillatory experiment. These are summarized in Figures 1 and 2.

Equipment and Procedure

The polymers were fed into a 1-in. Modern Plastics Machinery screw extruder which has been described in an earlier paper.[19] The melt was then forced through screens into a metering pump and a monofilament spinneret whose capillary had diameters from 0.03 to 0.10 in. and L/D ratios of 5 to 10. The molten polymer was then pulled downward by a multispeed take-up device. The take-up devices were driven by a 0–4000 rpm variable speed motor operated by a Heller controller. The molten fiber was then pulled through an electrically heated chamber containing two $6 \times {}^3/_4$-in. glass windows. Two types of take-up devices were used. One was a spool type on which the fiber was wound up. The second device consisted of two spools, one electrically driven and the other spring loaded so that tension could be applied to the fiber and the fiber pulled between the spools without being wound up on the take-up. The one spool could only be used on the polyethylene. The second spool device could be used for either the polyethylene or the polystyrene. All of the polystyrene was taken up with this two-spool device. The basic equipment is outlined in Figure 3.

Tensions in the descending fiber were measured with a Rothschild tensiometer utilizing a 0–10 g measuring head. In using this instrument,

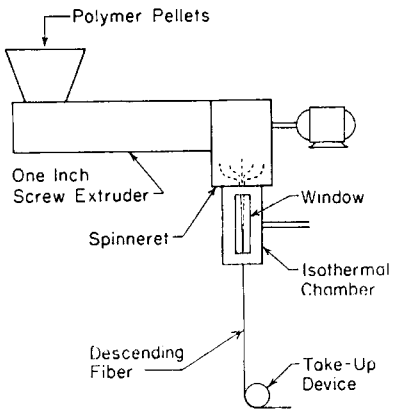

Fig. 3. Diagram of isothermal fiber spinning operation.

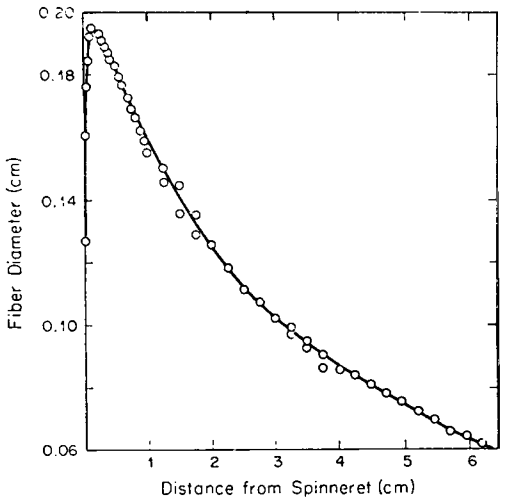

Fig. 4. Fiber diameter as a function of distance from the spinneret for a polyethylene run at 160°C.

one is limited by the size of the fibers on which the tension can be measured. The mass flow rate was determined for a run by dividing the weight of the fiber produced by the time involved.

Photographs were taken of the fiber descending through the heated chamber in order to analyze isothermal spinning. A 35-mm camera with fine grain film (fs 3.5, s.s. $^1/_{1000}$ sec) was used to take the photographs with an enlargement varying from 1/1 to 2/1 depending upon the experiment. The negatives were blown up (by a factor of 200/1 to 400/1) on a grid screen using a slide projector, and the diameter $d(x)$ of the fiber at increasing distances from the spinneret was measured (see Fig. 4).

About 50 runs at 160°C, 180°C, and 200°C were made for the isothermal spinning experiment.

RESULTS AND DISCUSSION

From Q and $d(x)$ data, the velocity $V(x)$ and velocity gradient dV/dx were computed. Typical results are shown in Figure 5. From the tensiometer results for F_L, $A(x)$, and eq. (2), the tensile stress $\sigma_{xx}(x)$ could be similarly evaluated (see Fig. 6). Drag forces on the fiber were found to be small when calculations were made using equations in the literature.[18,34] Surface tension forces and inertial contributions were negligible.

The first attempt at interpretation of data was to evaluate χ from eq. (5a) and plot it as a function of dV/dx. Several data points could be obtained from each run. The results are summarized in Figures 7 and 8. Values of three times zero shear viscosity are indicated on the plots. If the melts were Newtonian fluids, χ would simply be 3η. This was seen rather strikingly not to be the case. For polyethylene, data were ob-

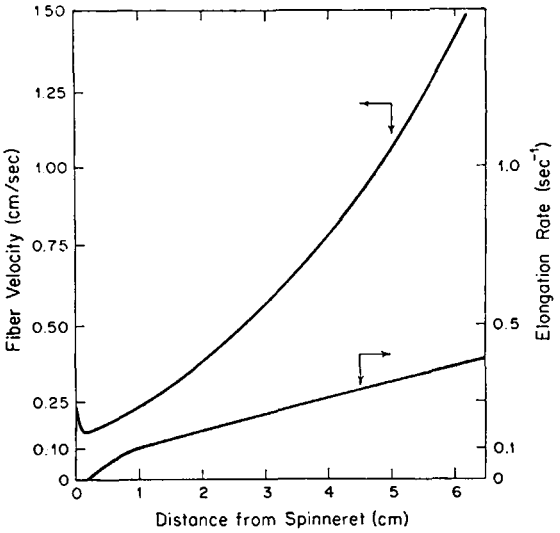

Fig. 5. Velocity and elongation velocity gradient as a function of distance from the spinneret for polyethylene at 160°C.

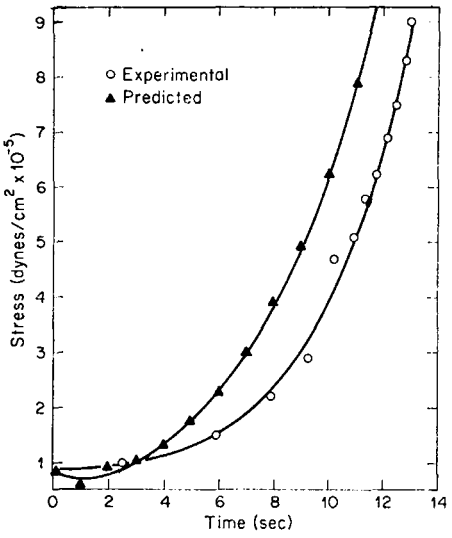

Fig. 6. Predicted stress vs. time using the Lodge theory ($G(t)$ obtained from the rheogonimeter) and experimental stress vs. time for polyethylene at 160°C.

tained in the range of 0.1 to 1.0 sec^{-1}. The χ value increases strikingly with dV/dx, which more or less agrees with the conclusions of Cogswell.[11] For low dV/dx, χ seems to approach 3η. Elongational viscosities for polystyrene were measured in the range of 0.03 to 2.0 sec^{-1}. The elongational viscosities for these melts were found to decrease with dV/dx. The decreasing χ value was also surprising from the viewpoint of rheological theory,

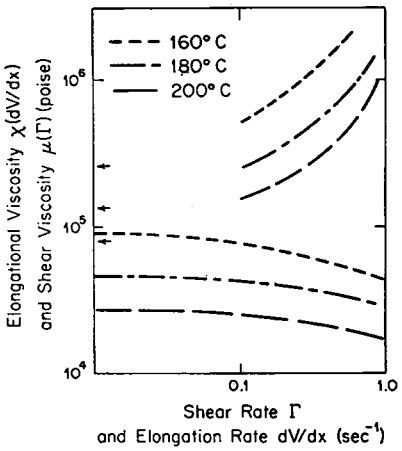

Fig. 7. Elongation viscosity of polyethylene.

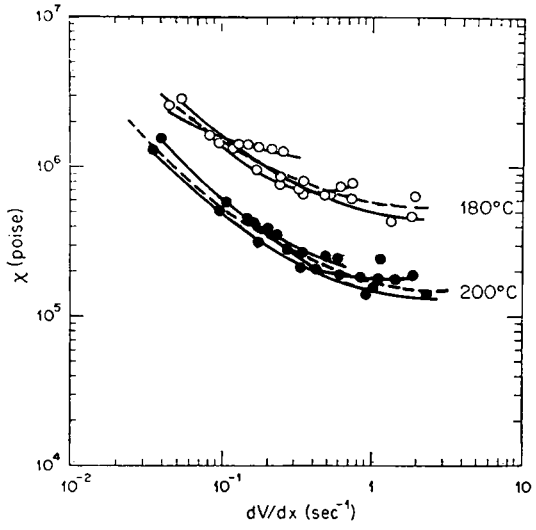

Fig. 8. Elongation viscosity of polystyrene.

for the second-order fluid predicts that the elongational viscosity should increase with extension rate.[12]

Considerable scatter was obtained in the χ-versus-dV/dx plots. When a polynomial was fit to the χ-versus-dV/dx data, an average per cent deviation was found of about 40% for the polyethylene data and about 15% for the polystyrene (see Table I). The large changes in dV/dx with x and in particular the polyethylene data suggested to us that a more sophisticated application of rheological theory might be justified. It was therefore decided to attempt to analyze experimental data in terms of the Lodge fluid theory outlined earlier in this paper, specifically eqs. (7) and (8).

TABLE I
Agreement of Various Rheological Theories with Stress Development Along the Streamline

Polymer	Temp., °C	Percent deviation, %[a]		
		Arbitrary elongational viscosity χ	Lodge model arbitrary $G(t)$ (form generally taken as $Ge^{-t/\tau}$)	Lodge model $G(t)$ determined from rheogoniometer
Polyethylene	160	27.4 (7)	28.0 (8)	89.1 (8)
Polyethylene	180	37.7 (6)	74.6 (5)	242 (4)
Polyethylene	200	55.4 (8)	24.9 (7)	80.3 (7)
Polystyrene	180	16.3 (3)	14.3 (3)	79.7 (3)
Polystyrene	200	13.4 (3)	16.0 (3)	6250 (3)

[a] Figures in parentheses indicate the number of runs.

The situation near the beginning of the spinline was interpreted as a long-duration, fully developed Poiseuille flow which continues until the maximum bulge, at which point the kinematics change to pure elongational kinematics. Two different approaches were taken to apply this deformation history to σ_{xx}-versus-x data. First, one might presume an expression for $G(t)$; substitute it into eq. (8) and then find the best form of this relation which fits the data. We have taken

$$G(t) = Ge^{-t/\tau_m}, \tag{9}$$

where τ_m is the maximum relaxation time, and then utilized it in this manner to determine G and τ_m. In some cases, two exponential terms were used (see Table II). In carrying out this analysis, we have taken the first term on the right-hand side of eq. (8) to be

$$\sigma_{xx}(0)e^{-t/\tau_m}.$$

The $G(t)$ values determined from the different runs were plotted together. This would be the equivalent of our χ as a function of dV/dx from the same runs. The results are shown in Table II and Figures 9 and 10. Considerable scatter may be seen, but this may be due to the fact that fiber spinning is a bad, i.e., insensitive, way of measuring $G(t)$ as one is relating an integral of this function to get the stress. Furthermore, eq. (9) is probably not a good representation of the materials' true behavior.

Since we have obtained dynamic viscosity data from the Weissenberg rheogoniometer, we may compute $G(t)$ from this data by fitting $\eta'(\omega)$ with[35]

$$\eta'(\omega) = \sum_{i=1}^{i=\infty} \frac{G_i\tau_i}{1 + \omega^2\tau^2} \sim \frac{G_1\tau_1}{1 + \omega^2\tau_1^2} + \frac{G_m\tau_m}{1 + \omega^2\tau_m^2} \tag{10}$$

and obtaining the best set of constants (G_1, G_m, τ_1, and τ_m). This may be compared with the $G(t)$ determined with $\sigma_{xx}(x)$ data as shown in Figures 9 and 10. The agreement is generally reasonable though not exceptionally good.

TABLE II
$G(t)$ Parameters from Fiber Spinning and Rheogoniometer

Polymer	Temp., °C	Fiber spinning				Rheogoniometer			
		G_m	τ_m	G_1	τ_1	G_m	τ_m	G_1	τ_1
Polyethylene	160	12,000	3.3	—	—	10,600	5.5	143,000	0.219
Polyethylene	180	15,000	1.9	—	—	11,300	3.0	150,000	0.0674
Polyethylene	200	7,500	2.0	40,000	0.25	9,000	2.2	70,000	0.1
Polystyrene	180	40,000	7.5	—	—	56,500	1.15	605,000	0.063
Polystyrene	200	20,000	6.5	—	—	33,000	0.3785	567,500	0.983

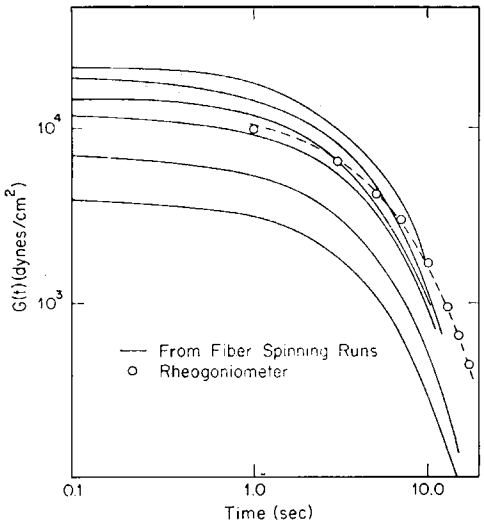

Fig. 9. Experimental relaxation moduli determined from rheogonimeter and fiber spinning for low-density polyethylene at 160°C.

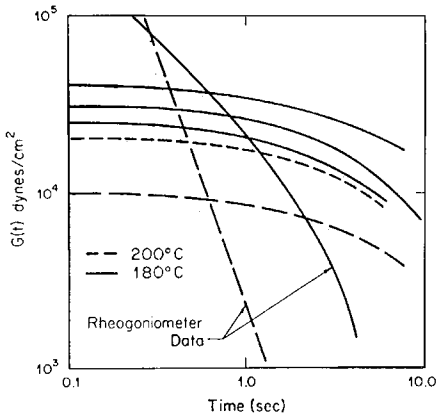

Fig. 10. Experimental relaxation moduli determined from rheogonimeter and fiber spinning for polystyrene.

A second way of looking at this problem is that we should be able to predict the stress along the spinline directly from the kinematics and the rheogoniometer dynamic data, i.e., G_1, G_m, τ_1, and τ_m are evaluated and $\eta'(\omega)$ and eq. (9) are substituted into eq. (8) and integration carried through to obtain σ_{xx}. Figure 6 contains a plot of theoretical predictions and experimentally determined values of σ_{xx} along the streamline for a typical polyethylene run.

Finally, we have contrasted the fit of $\sigma_{xx}(x)$ data with (1) rheogoniometer $\eta'(\omega)$ data and the Lodge fluid model, eq. (8); (2) mean $G(t)$ as determined from various fiber spinning runs and the Lodge fluid model, eq. (8); and

(3) mean $\chi(dV/dx)$ from fiber spinning and eq. (5a). The results are summarized in Table I. The Lodge fluid with arbitrary $G(t)$ gives perhaps a marginally better fit of the data than the use of an arbitrary χ function. Use of the Lodge fluid and a rheogoniometer-determined $G(t)$ gave by far the worse fit. For more details see the thesis of Dalton.[36]

Certainly more work needs to be done here. Our group is currently studying improved representations of the kinematics and utilization of more sophisticated constitutive equations. Additional spinning experiments are to be carried out on more thoroughly rheologically characterized polymers.

HEAT TRANSFER

Theoretical Analysis

Consider a molten polymer filament descending from a spinneret surface to a take-up roll. If radial temperature gradients within the fiber are neglected,[5,17] the filament temperature T_f at position x is determined by

$$\rho_f C_f A V \frac{dT_f}{dx} = 2\pi R h(T_f - T_\infty) + q_{\text{rad}} \tag{11}$$

with initial condition $T_{f(0)} = T_{f0}$, where h is the heat transfer coefficient for the cooling of the fiber and q_{rad} is the radiative heat transfer. The situation is more complicated when radial temperature gradients must be considered and when crystallization occurs. The former problem is discussed by Ziabicki[18] and the latter by Morrison.[37] However, these effects need not be considered here. Equation (11) may in the absence of radiation be directly integrated to give the temperature profile along the length of the fiber:

$$\frac{T_f - T_\infty}{T_{f0} - T_\infty} = \exp - \int_0^x \frac{2Rh}{\rho_f c_f A V} dx. \tag{12}$$

The central problem in the study of the cooling of fibers during spinning should be seen to be the determination of the heat transfer coefficient h.

The heat transfer coefficient connects the temperature at the fiber surface with the temperature profile in the ambient air through

$$\frac{q_{\text{rad}}}{2\pi R} + h(T_f - T_0) = - k \frac{\partial T}{\partial r}(R,x). \tag{13}$$

If one presumes radial symmetry, the temperature field in the ambient air is given by

$$u \frac{\partial T}{\partial x} + v \frac{\partial T}{\partial r} = \alpha \left[\frac{1}{r} \frac{\partial}{\partial r} \left(r \frac{\partial T}{\partial r} \right) + \frac{\partial^2 T}{\partial_x x^2} \right] \tag{14}$$

where α is the thermal diffusivity. Solution of this partial differential equation is necessary to obtain the heat transfer coefficient. To proceed,

we must specify boundary conditions and the velocity field. These will depend upon the detailed design of the equipment and, in particular, whether or not air is blown parallel or perpendicular to the filament. In our equipment, the fiber descends through the quiescent air of the laboratory. This allows us to specify $T(\infty,x)$ as being T_∞ and to write the Navier-Stokes equation for the ambient air as

$$u\frac{\partial u}{\partial x} + v\frac{\partial u}{\partial r} = \frac{\nu}{r}\frac{\partial}{\partial r}\left(r\frac{\partial u}{\partial r}\right) + g\beta(T - T_\infty) \tag{15}$$

where symmetry has been used to delete the θ component and a boundary layer approximation has been utilized to neglect the x component of the viscous forces. The term $g\beta(T - T_\infty)$ represents buoyancy forces. The u and v components are related by the continuity equation

$$\frac{\partial u}{\partial x} + \frac{1}{r}\frac{\partial}{\partial r}(rv) = 0. \tag{16}$$

The boundary conditions on u and v are

$$\begin{aligned} u(R,x) &= V \qquad u(\infty,x) = 0 \\ v(R,x) &\cong 0 \qquad v(\infty,x) = 0 \end{aligned} \tag{17}$$

The solution of this system of equations will indeed be very complex, even in the case where buoyancy may be neglected and the motion assured to be laminar. Heat transfer to a developing boundary layer moving in an axial direction over a cylinder held at constant temperature has been considered by Seban and Bond,[38] and natural convection heat transport from a cylinder held at constant temperature, by Sparrow and Gregg.[39] Simultaneous natural and forced convection near a vertical flat plate has been analyzed by Acrivos.[40] (No solution for cylinders has appeared.) However, as first pointed out by Sakiadis,[34] there is a fundamental difference between the classical boundary layer and the velocity field around a continuously generated surface. Tsou, Sparrow, and Goldstein[41] have considered heat transfer from a continuously generated sheet, and Griffith,[42] Rotte and Beek,[43] and Vasudevan and Middleman[44] have developed solutions for the heat transfer coefficients of cooling fibers. Only the work of Vasudevan and Middleman is, however, of interest to our need to obtain an expression for the heat transfer coefficient. Here, we will make three contributions to this problem. First, we will utilize the methods of dimensional analysis to obtain the form expected for h. Then we will give a new boundary layer analysis to compute it. Finally, in succeeding sections an experimental program will be described which results in a correlation for the heat transfer coefficient.

Dimensional Analysis

Let us introduce a characteristic velocity V (fiber velocity—we neglect diameter changes in the filament hereafter), lengths L (distance from the

spinneret to a point on the fiber), and R. After integration of the continuity equation and use of the axial temperature profile in the fiber, we may write the Navier-Stokes and energy equations in dimensionless form as follows:

$$u^* \frac{\partial u^*}{\partial x} - \frac{1}{r^*}\left(\frac{\partial u^*}{\partial r^*}\right)\int_{r^*=1}^{r}\left(\frac{\partial u^*}{\partial x^*}\right) r^* dr^* = \frac{\nu L}{VR^2}\left[\frac{1}{r^*}\frac{\partial}{\partial r^*}\alpha^* \frac{r^*}{u^*}\right] + \frac{g\beta(T_{f0} - T_\infty)L^3}{\nu^2}\cdot\left(\frac{\nu}{LV}\right)^2 \theta\, e^{-Mx^*}\Bigg] \quad (18)$$

$$u^* \frac{\partial}{\partial x^*}[\theta e^{-Mx^*}] - \frac{1}{r^*}\frac{\partial}{\partial r^*}(\theta e^{-Mx^*})\int_{r^*=1}^{r^*}\left(\frac{\partial u^*}{\partial x^*}\right) {}^*dr^* = \frac{\alpha L}{R^2 u}\frac{1}{r^*}\frac{\partial}{\partial r^*}\left[r^*\frac{\partial}{\partial r^*}(\theta e^{-Mx^*})\right] \quad (19)$$

where x^* is made dimensionless with L and r^* with R. Furthermore,

$$M = \frac{2\pi RH}{\rho_f c_f A V}$$

$$\theta = \frac{T(r,x) - T_\infty}{T_f - T_\infty}. \quad (20)$$

The dimensionless heat transfer coefficient is the Nusselt number given by

$$N_{\mathrm{Nu}} = \frac{hR}{k} = -\left(\frac{\partial \theta}{\partial r^*}\right)(x^*, r^* = 1.) \quad (21)$$

Using the classical methods of dimensional analysis (see Goldstein[22]), u^* may be expressed as a function of x^*, r^*, θ, M, (L/R), and the Reynolds, Prandtl, and Grashof numbers N_{Re}, N_{Pr}, and N_{Gr}:

$$N_{\mathrm{Re}} = \frac{LV}{\nu}; \quad N_{\mathrm{Pr}} = \frac{\nu}{\alpha}; \quad N_{\mathrm{Gr}} = \frac{g\beta(T_{f0} - T_\infty)L'^3}{\nu^2}. \quad (22)$$

In the Grashof number, the characteristic length L' is measured vertically upward. The Nusselt number may be similarly shown to be given by

$$N_{\mathrm{Nu}} = N_{\mathrm{Nu}}\left[N_{\mathrm{Re}}\left(\frac{R}{L}\right)^2, N_{\mathrm{Pr}}, \frac{g\beta(T_0 - T_\infty)L'^3}{\nu^2}, \frac{L'}{L}, \frac{\rho_f c_f}{\rho c}\right). \quad (23)$$

If there is little variation in the thermal properties of the polymers considered and all experiments are carried out in air, this may be reduced to

$$N_{\mathrm{Nu}} = N'_{\mathrm{Nu}}\left[N_{\mathrm{Re}}\left(\frac{R}{L}\right)^2, \frac{g\beta(T_0 - T_\infty)L'^3}{\nu^2}, \frac{L'}{L}\right]. \quad (24)$$

Boundary Layer Analysis

We shall outline an integral momentum analysis of this problem. An integral momentum study of boundary layer development along a contin-

uously generated cylinder was originally given by Sakiadis,[34] and an integral study, though of limited sort, for interphase transport was considered by Griffith,[42] The integral energy equation may be obtained by integration of eq. (14) with neglect of the axial conduction term. The equation obtained is

$$\rho cV \frac{d}{dx} \int_0^\delta 2\pi ru(T - T_\infty)dr = -k2\pi R \left(\frac{\partial T'}{\partial r}\right)_{r=R}. \tag{25}$$

Introducing θ of eq. (20), we presume the Sakiadis velocity profile and

$$\theta = 1 - \frac{1}{\beta'} \ln\left(1 + \frac{y}{R}\right). \tag{26}$$

The thermal boundary layer thickness Δ and the momentum boundary layer thicknesses δ are found to be

$$\delta = R(e^\beta - 1) \qquad \Delta = R(e^{\beta'} - 1) \tag{27}$$

where the quantity β' is given by

$$\frac{R^2V}{\nu}\left[\frac{d\beta'}{dx}\left(\frac{e^{2\beta}}{4\beta'^2}\left[1 - \frac{1}{\beta}\right] + \frac{1}{4\beta'^2}\left[1 + \frac{1}{\beta}\right]\right) + \frac{d\beta}{dx} \times \left(\frac{e^{2\beta}}{2\beta\beta'} + \frac{1 - e^{2\beta}}{4\beta^2\beta'} - \frac{e^{2\beta} - 1}{4\beta^2}\right)\right] = N_{\mathrm{Pr}} \frac{1}{\beta'}. \tag{28}$$

β is given by Sakiadis. The Nusselt number may be shown to be

$$N_{\mathrm{Nu}} = \frac{hR}{k} = \frac{1}{\beta'} \tag{29}$$

where β' is a function of $R^2V/\nu x$ or $N_{\mathrm{Re}}\,(R/x)^2$ and N_{Pr}. We have numerically solved eq. (28) coupled with the equivalent equations for the hydrodynamic boundary layer given by Sakiadis.

These results have been contrasted with the solution of the same problem by Vasudevan and Middleman. At lower Reynolds numbers ($x\nu/R^2V$ greater than 50), the Nusselt numbers of our solution are about 15% lower than the results of these authors. For higher Reynolds numbers, our Nusselt numbers are considerably lower than those of Vasudevan and Middleman.

EXPERIMENTAL

Materials

Four polymers were used in this study. These included the polyethylene and polystyrene used in the isothermal spinning experiment and two additional polystyrene melts. These were Dow Styron 666 whose rheological characteristics were described in an earlier paper,[19] and a Dow Styron 678. The molecular weight distributions of these polymers are not pertinent to

this study. However, they have been obtained and will be given in the forthcoming thesis of Salladay.[33]

Equipment and Procedure

In the heat transfer studies, no heated chamber was utilized and the fiber was pulled from the Modern Plastics Machinery screw extruder through stagnant air at 20–25°C. Temperature measurements were made along the length of the fiber using a Thermodot infrared pyrometer in the upper part of the spinline near the spinneret and a Hastings-Raydist contact pyrometer in the lower portion. The Thermodot has to be used on large fibers since it is necessary for the object to cover completely the field of view. This limits the fiber diameter at points of measurement to 0.15 cm or greater. It is necessary to know the emissivity for the descending molten filament to use the Thermodot. The emissivities for polyethylene and polystyrene were obtained experimentally by calibrating against known fiber temperatures. The Hastings-Raydist contact pyrometer used in the lower portion of the spinline also had its problems, for if the fiber was molten it would stick to the sensing device, and if the temperature was below 100°C there was a loss of sensitivity. Temperature profiles determined from using both the Thermodot and the H-R pyrometers do not show discontinuities.

The fiber kinematics were determined as in the isothermal spinning experiments.

Twenty-four runs with melt emerging from the spinneret at 200°C (22 runs) and 180°C (2 runs) were carried out to study heat transport.

RESULTS AND DISCUSSION

Typical temperature–distance plots for the polystyrene and the polyethylene are given in Figure 11. The polyethylene data show the effects of the heat of crystallization. A temperature plateau in the range of 130–135°C was observed. It was also clearly observed that increasing the elongation rate near the crystallization temperature increases the plateau temperature. In a run with a low dV/dx, the plateau value was 130°C. When this was increased to an effective local elongation rate (dV/dx) of 0.22 sec^{-1}, this temperature rose to 133°C and at an elongation rate of 0.50 sec^{-1}, to 135°C. The phenomenon of deformation increasing the rates of crystallization and indeed the equilibrium melting temperature has long been observed in stretching vulcanized rubber[45] and polymer melts[46,47,48] as well as in shearing flows of melts.[49] Justification by statistical mechanical arguments exists.[50,51,52]

The effect of radiation on the total rate of heat transfer has been taken into account and subtracted out [see eq. (11)] before evaluation of the heat transfer coefficient. Radiation accounts for approximately 20% of the total heat loss near the spinneret and 10% as the fiber approaches 100°C.

Figure 12 contains a plot of the local Nusselt number hR/k as a function of local Reynolds number $R^2V/\nu x$. The maximum value of the length

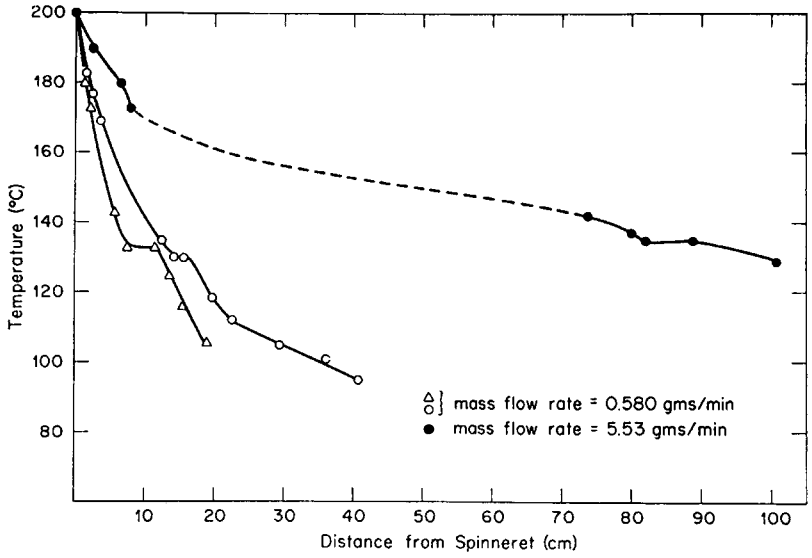

Fig. 11. Temperature profiles in polyethylene fibers.

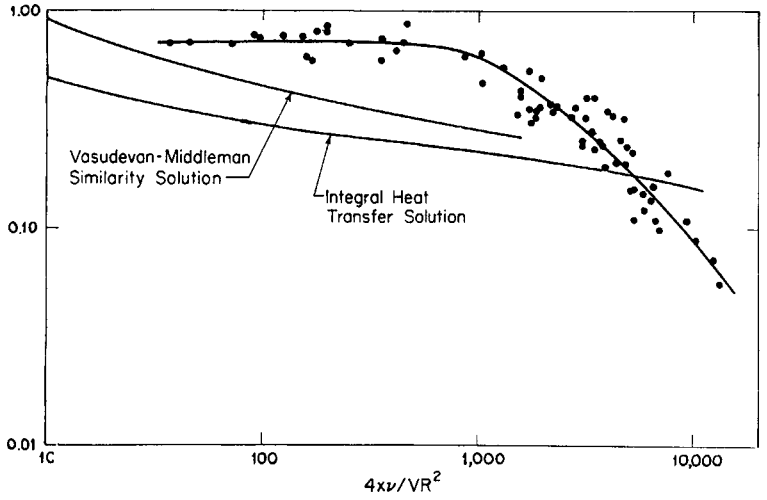

Fig. 12. Nusselt number vs. $4x\gamma/VR^2$.

Reynolds number xV/ν used is close to 20,000. As Griffith found the transition from laminar to turbulent flow for wet-spun fibers is about 100,000,[42] we would expect our data to be within the laminar range. Also contained in this figure are the theoretical curves for the boundary layer analysis given earlier. The lack of agreement is disappointing. It might be due to differences in boundary conditions such as fiber diameter variation. For values of $x\nu/R^2V$ below 750, the measured Nusselt numbers are larger than predicted, while for $x\nu/R^2V$ greater than 1000, the Nusselt

numbers become smaller. For $x\nu/R^2V$ less than 240, the Nusselt number becomes constant.

It was of some concern whether there are significant natural convection effects in the data. A regression analysis was carried out for an expression relating the Nusselt number to a sum of term linear in the fiber Reynolds number and a second term proportional to the $^1/_4$ power of the Grashof number. Almost no improvement in the heat transfer correlation was found by including the term in the Grashof number. In fact, the proportionality constant of this term was found to be negative.

The data of Kase and Matsuo[5] agree well with our own. Those of Wilhelm[6] and Ishibashi, Aoki, and Ishii[7] are somewhat higher. Ishibashi et al.'s data are at high-length Reynolds numbers (70,000–210,000), and this may indicate turbulent rather than laminar flow. We are not certain of the reasons for the deviation of Wilhelm's data. Some type of spinning chamber may well have been used. This might explain the difficulties. The different thermal properties of polyester as opposed to hydrocarbon melts could be of significance.

We have correlated our data with the following equations:

$$\begin{aligned} N_{\mathrm{Nu}} &= 0.72 \qquad \frac{x\nu}{R^2V} < 200 \\ N_{\mathrm{Nu}} &= 9.45 N_{\mathrm{Re}}{}^{1/2}\left(\frac{R}{x}\right) \qquad 200 < \frac{x\nu}{R^2V} < 500 \\ N_{\mathrm{Nu}} &= 200 N_{\mathrm{Re}}\left(\frac{R}{x}\right)^2 \qquad \frac{x\nu}{R^2V} > 500. \end{aligned} \tag{30}$$

CONCLUSIONS

An experimental study of the melt spinning of fibers has been carried out. The study was in two parts: (1) isothermal spinning, and (2) heat transfer. Elongational viscosity and a nonlinear viscoelastic integral theory approaches were used to correlate kinematic and tensiometer force data in the former study. The integral theory seems to yield a better correlation. Both a new theory of heat transport from fibers was outlined and a new experimental correlation for the Nusselt number was obtained in the second study.

Professor D. C. Bogue was involved in the initial stages of this work. However, because of a Visiting Professorship at Kyoto University from January to September 1970, he was unable to engage in the later parts of this effort. We thank him though for is comments and encouragement.

We would like to thank Professor J. E. Spruiell, Dr. I. J. Chen, and G. E. Hagler for their helpful comments throughout the course of this work. D. G. Salladay of our group determined the molecular weight distributions of some of the polymers involved. The Dow Chemical Company supplied the polymers used in this study and cooperated with us in their characterization. We wish to thank them for their cooperation. One of us (J. N. D.) received the aid of a fellowship from the Tennessee Eastman Company.

References

1. W. Carothers and J. W. Hill, *J. Amer. Chem. Soc.*, **54**, 1579 (1932).
2. E. K. Bolton, *Ind. Eng. Chem.*, **34**, 53 (1942).
3. A. Ziabicki and K. Kedzierska, *Kolloid-Z.*, **171**, 51 (1960).
4. A. Ziabicki, *Kolloid-Z.*, **175**, 14 (1961).
5. S. Kase, and T. Matsuo, *J. Polym. Sci. A.*, **3**, 2541 (1965).
6. G. Wilhelm, *Kolloid-Z. Z. Polym.*, **208**, 97 (1966).
7. T. Ishibashi, K. Aoki, and T. Ishii, *J. Appl. Polym. Sci.*, **14**, 1597 (1970).
8. F. T. Trouton, *Proc. Roy. Soc., Ser. A.*, **77**, 426 (1906).
9. A. Kaye and D. G Vale, *Rheol. Acta*, **8**, 1 (1969).
10. R. L. Ballman, *Rheol. Acta*, **4**, 138 (1965).
11. F. N. Cogswell, *Rheol. Acta*, **8**, 187 (1969).
12. J. L. White, *J. Appl. Polym. Sci.*, **8**, 2339 (1964).
13. M. A. Matovich, and J. R. A. Pearson, *Ind. Eng. Chem., Fundam.*, **8**, 512 (1969).
14. C. D. Han, *Rheol. Acta*, **9**, 355 (1970).
15. A. Ziabicki, and K. Kedzierska, *J. Appl. Polym. Sci.*, **2**, 14, 24 (1959); *ibid.*, **6**, 111, 361 (1962).
16. K. Katayama, T. Amano and K. Nakamura, *Kolloid Z.-Z. Polym.*, **226**, 125 (1968).
17. A. Ziabicki, *Appl. Polym. Symposia*, **6**, 1 (1967).
18. A. Ziabicki, in Man-Made Fibers, Vol. 1, H. Mark, S. M. Atlas, and E. Cernia, Eds., Interscience, New York, 1967.
19. T. F. Ballenger, I. J. Chen, J. W. Crowder, G. Hagler, D. C. Bogue, and J. L. White, *Trans. Soc. Rheol.*, **15** 195 (1971).
20. G. A. Bialas and J. L. White, *Rubber Chem. Technol*, **42**, 675, 682, 691 (1969).
21. T. F. Ballenger and J. L. White, *Chem. Eng. Sci.*, **25**, 1191 (1970), and *J. Appl. Polym. Sci.*, in press.
22. S. Goldstein, *Modern Developments in Fluid Dynamics*, Clarendon Press, Oxford, 1938.
23. D. C. Bogue, and J. L. White, *Engineering Analysis of Non-Newtonian Fluids*, NATO Agardograph 144 (1970). Available from NTIS Springfield, Virginia as Document AD-710-324.
24. B. D. Coleman and W. Noll, *Phys. Fluids*, **5**, 840 (1962).
25. A. B. Metzner, J. L. White and M. M. Denn. AIChE J. **12**, 863 (1966).
26. J. L. White and N. Tokita, *J. Appl. Polym. Sci.* **11**, 321 (1967).
27. I. J. Chen, and D. C. Bogue, *Trans. Soc. Rheol.*, in press.
28. I. J. Chen, Ph.D. Dissertation, Department of Chemical and Metallurgical Engineering, University of Tennessee, Knoxville, 1971.
29. A. S. Lodge, Trans. Faraday Soc., **52**, 120 (1956).
30. A. S. Lodge, *Elastic Liquids*, Academic Press, New York, 1964.
31. J. L. White, *Rubber Chem. Technol.*, **42**, 257 (1969).
32. J. L. White, *Rubber Chem. Technol.*, **42**, 691 (1969).
33. D. G. Salladay, unpublished research to be contained in forthcoming M.S. Thesis in Chemical Engineering, University of Tennessee, Knoxville.
34. B. C. Sakiadis, A.I.Ch.E. J., **7**, 26, 221, 467 (1961).
35. J. D. Ferry, *Viscoelastic Properties of Polymers*, 2nd ed., Wiley, New York, 1970.
36. J. N. Dalton, M.S. Thesis in Chemical Engineering, University of Tennessee, Knoxville, 1971.
37. M. E. Morrison, *A.I.Ch.E. J.*, **16**, 57 (1970).
38. R. A. Seban, and R. Bond, *J. Aero. Sci.*, **19**, 671 (1961).
39. E. M. Sparrow, and J. L. Gregg, *Trans. ASME*, **78**, 1824 (1956).
40. A. Acrivos, *A.I.Ch.E. J.*, **4**, 285 (1958).
41. F. K. Tsou, E. M. Sparrow, and R. J. Goldstein, *Int. J. Heat Mass Transfer*, **10**, 219 (1967).

42. R. M. Griffith, *Ind. Eng. Chem., Fundam.*, **3**, 245 (1964).
43. J. W. Rotte, and W. J. Beek, *Chem. Eng. Sci.*, **24**, 705 (1969).
44. G. Vasudevan, and S. Middleman, *A.I.Ch.E. J.*, **16**, 614 (1970).
45. A. N. Gent, *J. Polym. Sci. A*, **3**, 3787 (1965); *ibid.*, **4**, 447 (1966).
46. D. E. McCord, and J. E. Spruiell, manuscript in preparation.
47. D. E. McCord, M.S. Thesis in Chemical Engineering, University of Tennessee, Knoxville, 1970.
48. A. B. Thompson, *J. Polym. Sci.*, **34**, 741 (1959).
49. T. Kawai, T. Matsumoto, M. Kato, and H. Maeda, *Kolloid-Z. Z. Polym.*, **222**, 1 (1968).
50. P. J. Flory, *J. Chem. Phys.*, **15**, 397 (1947).
51. M. Yamamoto and J. L. White, *J. Polym. Sci. A-2*, **9**, (1971).
52. W. R. Krigbaum, and R. J. Roe, *J. Polym. Sci. A*, **2**, 4391 (1964).

Received March 31, 1971
Revised May 28, 1971